URSI GASS 2020, Rome, Italy; 29 Aug. - 5 Sep. 2020

Structuring Wavefront via Curving a 3D-Printed Metasurface

He-Xiu Xu(1), Haipeng Li(1), Guangwei Hu(2), Cheng-Wei, Qiu(2)
(1) Department of Electronic Science & Technology, Air Force Engineering University, Xi'an, 710051, China
(2) Department of Electrical and Computer Engineering, National University of Singapore, Singapore 117583, Singapore

Abstract

Achieving kaleidoscopic wavefront controls on arbitrary curved platforms, especially in transmission case, is pivotal yet very challenging in the emerging technologies of communication and detection systems. Here, we propose and demonstrate a strategy to control the versatile transmissive structured wavefront on arbitrary conformal platform via curving a three-dimensional (3D) printed flexible metasurface. The conformal metasurface (CMS) is designed with broadband performance by cascading three super-thin flexible printed-circuit-boards and two 3D-printing substrates. A general strategy is theoretically proposed that projects arbitrary curved surface to a referenced plane via judiciously engineering the compensation of the curvature-induced phase. For verification, a proof-of-concept multifunctional conformal meta-device is designed, numerically and experimentally characterized. The curved meta-device is a full-cylinder CMS and is composed of four devices each conformed to a quarter cylinder and exhibited a distinguished angle-multiplexed functionality, i.e., generating highly-directive beam, vortex-beams carrying orbital angular momentums (OAMs) and dual-beam steering with different angular positioning. Our findings set up a robust, systematic, multifunctional and ultra-compact free-form metasurface for complete wavefront control over arbitrary curved platforms.

1. Introduction

The past decades have witnessed a rapid development of metasurfaces [1-6] (MSs) that provide powerful capability to reshape the wavefronts of electromagnetic (EM) waves regarding to their polarizations, amplitudes and frequencies. By engineering the proper meta-atoms with abrupt phase discontinuities, the MSs can effectively manipulate the EM waves in a super-thin and low-loss fashion, which can also be easily fabricated via the printed-circuit-board (PCB) technology in microwave region. To date, various exciting applications of MSs have been demonstrated, such as anomalous refraction/reflection, focusing, beamforming, vortex-beam generation, propagating wave to surface wave transformation, multi-beam wave generation, the directional Janus functionalities, and many others. Despite these flat profiles, MSs synthesized in the curved platforms could also be appealing considering their conformal nature for real-world applications. However, most of these conformal MSs (CMSs) are focused on reflected geometry to achieve the cloaking and scattering enhancement. The interference between incident and reflected light makes the reflected conformal MS more suitable for scattering cancellation-based cloaking but it seriously limits its applications in areas of lens, special beam generator and especially in multi-functional integration.

Nonetheless, conformal wavefront shaping in transmission scheme are still elusive and in infancy, from the perspective of both fundamental physics and experimental implementations. A numerical method was proposed, based on conformal boundary optics, to modify the finite difference time-domain (FDTD) approach for the accurate calculation of the electromagnetic fields across CMSs. However, only the theoretical boundaries for conformal perfect absorbing layer, beam deflector and curved meta-lens are provided, while no practical structures could be applied to realize such theoretical boundaries. In a different context, the convex and concave cylindrical lenses have been designed on a flexible dielectric MS, which is nothing new but traditional geometric optical elements, let alone its weak suitability for microwave wavefronts engineering as it is composed of silicon nano-posts embedded in an intrinsic flexible polymer substrate. In general, traditional transmissive MSs in microwave frequency band with multilayer structure are not easy to be conformal in arbitrary curved platforms.

In light of above, here we theoretically and experimentally propose a new kind of transmissive MSs composed by the meta-atom that relies on the 3D-printing technology. Herein, flexible MSs, made of two orthogonal gratings and central half-wave plates, are separated by two 3D-printing dielectric boards. This kind of meta-atom with orthogonal gratings exhibits a wide transparent window and own the ultrathin lateral profile of only $\lambda_0/6$, with λ_0 being the free-space wavelength at the operating frequency. Furthermore, the function of the outer layers endows this special kind of element with some tolerance of layer misalignment, making the meta-atom extremely robust for conformal design. By using the sophisticatedly designed meta-atom with the ability of complete phase manipulation, a ray-tracing phase compensation strategy are proposed based on the projection of the curved surface to a referenced plane, which one could further modify the phase for designed functionalities.

2. Concept and conformal design strategy

As the proof-of-concept demonstration on cylindrical platform, we achieve a CMS with kaleidoscopic functions in full space shown in Figure 1a. The full cylindrical CMS has four distinct functions, including the highly directive radiation pattern, single-mode and dual-mode vortex

beams and dual-beam steering, can be experimentally achieved in a single full CMS when excited by a monopole, manifesting the multifunctional, ultra-compact and synthesized feature.

The design of the CMS follows a four-step design flow shown in Figure 1b. Firstly, the points on the curved platform are projected to a suitably referenced plane so that the outing wave can be converted to be near-plane wave. Secondly, proper phase distributions are endowed on the projection-plane that could achieve the desired functionality such as vortex-beam and dual-beam generation. Thirdly, all the structural parameters for a CMS are determined and the samples are fabricated with 3D-printing technology. Lastly, the final MSs can be made along with the carefully chosen and settled proper feeding source. Moreover, we firmly believe our systematic and exhaustive studies here could open up the rarely explored avenue of the free-form multifunctional conformal meta-devices with the advanced feasible fabrication techniques that could optimistically promise the next-generation communication, detection and the defense technologies.

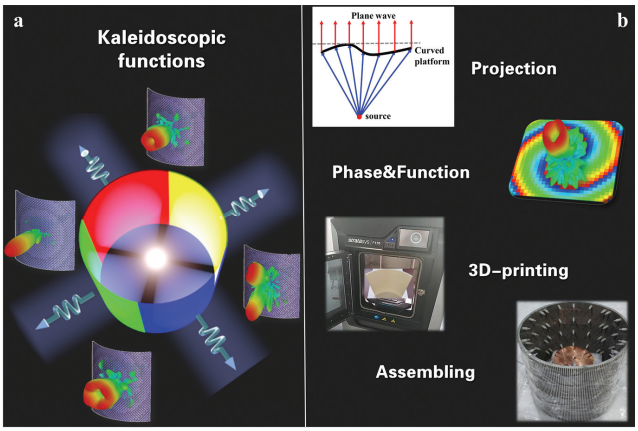

Figure 1. The schematic sketch and four-step design flow of the CMS with kaleidoscopic functions in full space. a) The schematic sketch of the total CMS. b) The four-step design flow. Projection: the points on the curved platform are projected to a suitably referenced plane so that the outing wave can be converted to be near-plane wave. Phase & Function: endowing the proper phase distributions on the projection-plane that could achieve the desired functionality such as vortex-beam and dual-beam generation. 3D-printing: endow all determined structural parameters to a CMS sample based on a direct printing. Assembling: the final MSs can be made along with a carefully chosen and fixed feeding source. Here, the process to design a multifunctional full-cylinder CMS with four beams of single-beam/dual-beam highly-directive patterns, single-mode/dual-mode vortex patterns are shown as an example.

The concept of the phase compensation is inspired by the ray-tracing approach by projecting the curved surface to a common referenced plane [5]. As illustrated in Figure 2a, and take the cylindrical surface for example, suppose that the EM waves emitted from an ideal point source (S) is applied on the cylindrical surface. The local point (O) on the surface is selected as the referenced point and M′ is its tangent surface. To firstly form a plane wave, the phase differences between the arbitrary optical path (from trace line SK to trace line KK′) and the referenced optical path (trace line SO) can be compensated by the properly placed meta-atoms on the curved surface. Thereafter, functions of the planar MSs can extend to the curved MSs. The optical paths of SO and SK-KK′ should satisfy the following equations:

$$\mathrm{SO}=R\ ;\ \mathrm{SK}=\sqrt{R^2+y^2}\ ;\ \mathrm{KK'}=R(1-\cos\gamma)\quad(1)$$

In the practical design, we first place the meta-atom on a flexible board, and then bend it onto the curved surface. Note that the azimuth angle (γ) and the abscissa on the flexible MS (x) is connected by $\gamma = x/R$. Therefore, the optical path difference will cause a phase difference $\varphi(x, y)$ written as:

$$\varphi(x,y)=\frac{2\pi}{\lambda}\left[R(1-\cos\frac{x}{R})+\sqrt{R^2+y^2}-R\right]\quad(2)$$

Thus, we can carefully place the meta-atoms with different transmission phases on the spatial domains of the flexible MS, to compenstate this phase difference for our designed CMSs.

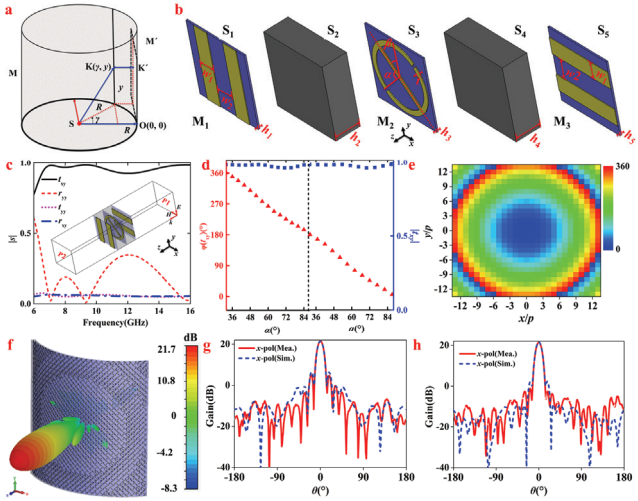

Figure 2. a) CMS with cylindrical platforms. Surface M indicates the curved platform while M′ is the tangent surface of M. Point S is the location of the ideal point source. O is tangent point of M′ and M. K is point on the curved surface while K′ is the projection of K on the referenced flat surface M′. R is the radius of the cylinder. b) Topology of the initial meta-atom. The following geometrical parameters are fixed: period of the unit cell is p = 5.8 mm, width of the metallic grating is w_1=1.3mm, gap between the two gratings is w_2 = 1.6mm, width of the metallic line of the modified I-shape particle is t = 0.4mm and the rotational angle is β = ±45° (anticlockwise is defined as the positive direction while clockwise as negative direction). The arc angle of the I-shape particle denoted by α is tuned appropriately in designing each element. c) Reflection and transmission coefficients under y-polarized incidence of the meta-atom with its simulated model. d) The curve of t_{xy} versus α with β = ±45°. e) Distribution mapping of φ_C on the flexible board of the highly-directive CMS. f) 3D far-field radiation pattern at 10 GHz. Simulated and measured far-field radiation patterns of the highly-directive CMS in g) *xoz*-plane and h) *yoz*-plane.

To fulfil the proposed strategy above, the meta-atom consisting of three metallic layers (marked as M_1, M_2 and M_3) are numerically studied as our meta-atoms (Figure 2b). Here, M_1 and M_3 are orthogonal gratings while M_2 is a circular I-shape particle. These three metallic layers are all printed on flexible teflon-glass-cloth-boards with thickness of 0.1 mm, dielectric constant (ε_r) of 2.65 and loss tangent ($\tan\delta$) of 0.003. Three flexible layers (S_1, S_3 and S_5) are sandwiched by 3D printing material ABS-M30 (S_2 & S_4), which exhibits thickness of 2 mm, $\varepsilon_r = 2.7$ and $\tan\delta = 0.005$. Thanks to the 3D printing and flexible dielectric board, CMSs with arbitrary shape and desired thickness can be easily fabricated.

For the orthogonal gratings, M_1 enables x-polarized wave to be largely transmitted and y-polarized waves reflected, whereas M_3 vice versa. Suppose a y-polarized EM wave is normally incident along z-direction, and the four scattering components should obey $|r_{xy}|^2 + |r_{yy}|^2 + |t_{xy}|^2 + |t_{yy}|^2 = 1$ due to the energy conservation. As is known, the grating along x-polarization (M_3) will prevent the reflection of x-polarized wave (r_{xy}) while the grating along y-polarization (M_1) will prevent the transmission of y-polarized wave (t_{yy}). Futhermore, the central metallic layer (M_2) functioning as a half-wave plate enables the conversion of most incident power to its cross-polarized component t_{xy}. As verified in Figure 2c, the transmission rate of t_{xy} is higher than 0.9 in a broad band. Next, we adjust the arm length ($l\alpha$) of the central particle to control $\varphi(t_{xy})$. As shown in Figure 3a and 3b, when α changes from 32° to 88°, the tuning range of $\varphi(t_{xy})$ reaches 180° with $|t_{xy}|$ better than 0.9 within 8~13.8 GHz. Meanwhile, when β changes from 45° to -45°, $\varphi(t_{xy})$ manifests a 180° phase jump while $|t_{xy}|$ remains unchanged. That implies the broadband complete phase control can be realized. As an example, the quasi-continuous phase tuning and near-unity amplitude at 10 GHz is shown in Figure 2d, where a 360° phase coverage with large transmission rate over 0.95 is achieved.

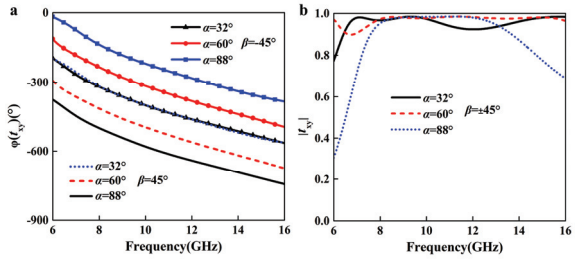

Figure 3. Wideband performance of the meta-atom. The curves of a) phase and b) amplitude versus frequency with $\alpha = 32°$, 60° 88° and $\beta = 45°$, -45°. Herein, $\alpha = 32°$, 60° and 88° are the minimum, center and maximum values of the parameter scanning range, respectively.

3. Full-cylinder CMS with assembled quad functionalities

Now, we intend to utilize aforementioned meta-atom with exotic feature to design novel meta-device with abundant functionalities. Here, we envisioned that the assembly of quad cylindrical regions could enable a single synthesized CMS for quad functionalities at different spatial angular positions, severing as the free-form full-space platform for the versatile wavefront manipulation. The arc length of the quarter cylindrical surface is $\pi R/2$ = 157 mm. Then the number of meta-atoms along x-axis on the planar MS is calculated as 27, and the MS is set to be square so that the number of meta-atoms along y-axis is also 27.

For spiral phase with OAM, the key is to introduce an azimuthal phase dependence $e^{-jl\varphi}$ into the EM wave, thus the phase of element located in (x', y') should be $\varphi(x', y')=l\tan(y'/x')$, where l is the topological charge of OAM mode. For cylindrical vortex plate, the point of (x', y') on the tangent plane of M′ corresponds to the point of K on the original planar MS. Therefore, x' and y' should satisfy $x'=R\tan(x/R)$ and $y'=y$. To achieve a cylindrical vortex plate, the phase compensation term should be rewritten as following:

$$\varphi_{vl}(m,n)=\frac{360}{\lambda}\left[R\left(1-\cos\frac{mp}{R}\right)+\sqrt{R^2+(np)^2}-R+l\tan^{-1}\left(\frac{y}{R\tan(\frac{x}{R})}\right)\right]$$
$$(m,\, n=0,\pm1,\cdots\pm13) \quad (3)$$

The inter-device communication plays an important roles in real-life problems such as the earth-space connections, which usually requires the dual beam steering to different directions. One proof-of-concept application of our CMS here targets to obtain such symmetric dual-beam deflections with oblique angles of ±30° along y-axis. For a beam steering, the gradient phase along y directions given as $\varphi(y)=\delta|y|$ should be added, where δ is the phase gradient of the double broken line shown in Figure 4a. The deflecting angle θ_b thus could be obtained according to the generalized refraction law:

$$\sin(\theta_b)=\frac{\lambda}{360}\times\frac{\delta}{p} \quad (4)$$

By inserting $\theta_b = 30°$, $\lambda = 30$mm and $p = 5.8$ mm into Eq. (4), δ is calculated as 34.8°. Then the final phase distribution of the dual-beam CMS should obey:

$$\varphi_d(m,n)=\frac{360}{\lambda}\left[R\left(1-\cos\frac{mp}{R}\right)+\sqrt{R^2+(np)^2}-R+34.8|n|\,p\right]$$
$$(m,\, n=0,\pm1,\cdots\pm13) \quad (5)$$

The calculated phase distribution is depicted in Figure 4b.

To form a a plane wave or a highly-directive beam, the discretized phase differences between the arbitrary optical path and the referenced optical path can be compensated by as the following

$$\varphi(m,n)=\frac{360}{\lambda}\left[R\left(1-\cos\frac{mp}{R}\right)+\sqrt{R^2+(np)^2}-R\right] \quad (6)$$
$$(m,\, n=0,\pm1,\cdots\pm13)$$

where m (n) is the number of meta-atoms in x (y) direction.

According to the phase distributions calculated based on above equations, α and β for each quater cylinder can be mapped out, respectively. To excite the entire cylindrical CMS, an omnidirectional feed source is necessary. In our design, a monopole operating around 10 GHz is adopted. The monopole as well as its far-field radiation pattern is shown in Figure 4e. The full cylindrical CMS is constructed in order to achieve the functions of single-mode vortex, dual-beam deflection, dual-mode vortex and highly directive pencil-beam, which are experimentally realized as shown in Figures 4f and 4g. Compared with four single CMSs, the gains is reduced because of the total

power is distributed to the four CMSs. For more details, two-dimensional polar radiation patterns on *xoz*-plane, *yoz*-plane and *xoy*-plane are shown in Figures 4h, 4i and 4j, respectively. And the excellent agreement between the measured and simulated results could be concluded. Thus, our strategy has shown that the on-demand multiple functionalities could be easily achieved and synthethized by a single conformal metasurface, which will be of great importance for the ultra-compact and multifunctional microwave technologies.

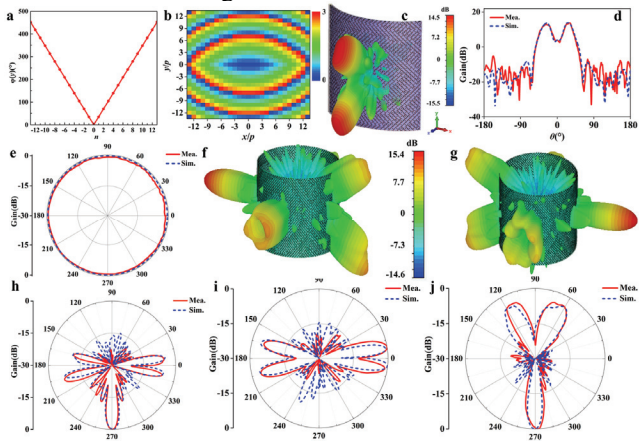

Figure 4. Performances of the dual-beam CMS and the full cylinder CMS. a) Phase curve along *y*-axis of the dual-beam CMS. b) The distributions of φ_d. c) 3D radiation pattern at 10 GHz. d) Simulated and measured far-field radiation patterns on *yoz*-plane. e) Far-field radiation pattern of the monopole with its prototype shown in the inset. 3D f) front-view and g) back-view radiation patterns of the entire CMS at 10 GHz. Simulated and measured far-field radiation patterns on h) *xoz*-plane, i) *yoz*-plane and j) *xoy*-plane.

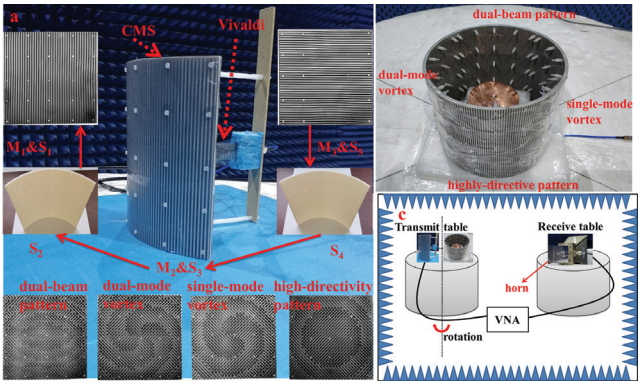

Figure 5. Photograph of the fabricated sample and experimental setup of the CMSs. a) Measurement of the single quarter CMSs with their assembling process. b) Measurement of the total CMS with the locations of each single CMS. c) Schematic diagram of the measurement.

In preparing our final samples, all metallic and flexible layers are fabricated with standard printed-circuit-board (PCB) and 3D printing technologies. The assembling process of the four quater CMSs is shown in Figure 5a. The flexible boards and 3D printing quarter-cylinder are assembled together with plastic screws. The four quarter-cylinder CMSs are assembled into a full cylindrical CMS by using tapes which is shown in Figure 5b. In our experiment, the schematic diagram of the measured surroundings is shown in Figure 5c. As is shown, the CMSs are placed on a transmit table and a wideband horn is placed on another received table. By rotating the transmit table automatically, the scattering powers of all the angles are received by the circularly polarized horn and recorded by a vector network analyzer (AV3672B).

4. Conclusion

To sum up, we theoretically proposed and experimentally demonstrated a new strategy by using flexible PCBs and 3D-printing boards to achieve wavefront shaping on arbitrarily curved platforms. We first analyze the transformation from curved face to flat surface by compensating the phase differences caused by the optical paths. Then, cylindrical platforms are chosen to verify the method. Four far-field patterns of highly-directive beam, vortex beams with topological charges of 1 and 2 and dual-beam are achieved on a quarter of cylindrical platform, respectively. Finally, the full-space spatially multiplexed applications with four different functions are simultaneously obtained in single synthesized curved metasurface, with the great promise of multifunctional, high-capacity and free-form meta-devices. Our findings offer a general strategy to achieve various wavefront shaping on arbitrary platforms in transmission cases which can be widely used in new generation of communication, detection and defense systems.

5. Acknowledgements

This work was supported by the Youth Talent Lifting Project of the China Association for Science and Technology (17-JCJQ-QT-003); Key Program of Natural Science Foundation of Shaanxi Province (2017KJXX-24); Aviation Science Foundation of China (20161996009).

6. References

[1] N. F. Yu, P. Genevet, M. A. Kats, F. Aieta, J.-P. Tetienne, F. Capasso, and Z. Gaburro, “Light propagation with phase discontinuities: generalized laws of reflection and refraction,” *Science* **334**, 2011, p. 333.

[2] H.-X. Xu, G. W. Hu, Y. Li, L. Han, J. L. Zhao, Y. M. Sun, F. Yuan, G.-M. Wang, Z. H. Jiang, X. H. Ling, T. J. Cui, C.-W. Qiu, “Interference-assisted kaleidoscopic meta-plexer for arbitrary spin-wavefront manipulation,” *Light: Sci. Appl.* **8**, 2019, p.3.

[3] H.-X. Xu, G. W. Hu, L. Han, M. H. Jiang, Y. J. Huang, Y. Li, X.M. Yang, X. H. Ling, L. Z. Chen, J. L. Zhao, C.-W. Qiu, “Chirality-assisted high-efficiency metasurfaces with independent control of phase, amplitude and polarization,” *Adv. Opt. Mater.* **7**, 2019, p. 1801479.

[4] L. Li, T. J. Cui, W. Ji, S. Liu, J. Ding, X. Wan, Y. B. Li, M. Jiang,C.-W. Qiu, S. Zhang, “Electromagnetic reprogrammable codingmetasurface holograms”, *Nat. Commun.* **2017**, *8*, 197.

[5] H.-X. Xu, S. Tang, C. Sun, L. Li, H. Liu, X. Yang, F. Yuan, and Y. Sun, “High-efficiency broadband polarization-independent superscatterer using conformal metasurfaces,” *Photonics Res.*, **6**, 2018, 8, pp. 782-788.

[6]Y. Ra’di, D. L. Sounas, and A. Alù, “Metagratings: Beyond the limits of graded metasurfaces for wave front control”, *PRL* **119**, 2017, 067404.